Scientific Reports

https://doi.org/10.1038/s41598-026-39722-x

Article in Press

Autism spectrum disorder-associated Sema5A p.Arg676Cys drives Arf6/FE65 signaling and aberrant cell morphogenesis

Received: 20 April 2025

Accepted: 6 February 2026

Published online: 17 February 2026

Cite this article as: Takahashi M., Yako H., Miyamoto Y. *et al.* Autism spectrum disorder-associated Sema5A p.Arg676Cys drives Arf6/FE65 signaling and aberrant cell morphogenesis. *Sci Rep* (2026). https://doi.org/10.1038/s41598-026-39722-x

Mikito Takahashi, Hideji Yako, Yuki Miyamoto, Mutsuko Kukimoto-Niino, Mikako Shirouzu & Junji Yamauchi

Autism spectrum disorder-associated Sema5A p.Arg676Cys drives Arf6/FE65 signaling and aberrant cell morphogenesis

Mikito Takahashi[1,2#], Hideji Yako[1,2#], Yuki Miyamoto[1,2,3], Mutsuko Kukimoto-Niino[4], Mikako Shirouzu[4], and Junji Yamauchi[1,2,5*]

[1]Laboratory of Molecular Neuroscience and Neurology and [2]Laboratory for Drug Target Discovery, Tokyo University of Pharmacy and Life Sciences, Hachioji, Tokyo 192-0392, Japan; [3]Department of Precision Medicine, National Research Institute for Child Health and Development, Setagaya, Tokyo 157-8535, Japan; [4]Laboratory for Protein Functional and Structural Biology, Center for Biosystems Dynamics Research, RIKEN, Tsurumi, Yokohama 230-0045, Japan; [5]Department of Biological Sciences, Tokyo College of Biotechnology, Ota, Tokyo 157-8535, Japan

[#]These authors equally contributed to this study

*Corresponding author: Junji Yamauchi

Laboratory of Molecular Neuroscience and Neurology

Laboratory for Drug Target Discovery

Tokyo University of Pharmacy and Life Sciences

1432-1 Horinouchi, Hachioji, Tokyo 192-0392, Japan

Email: yamauchi@toyaku.ac.jp

Tel: (+81)42-676-7164

Fax: (+81)42-676-8841

Abstract

Autism spectrum disorder (ASD) is a neurodevelopmental condition characterized by impairments in social interaction, challenges with communication, and repetitive behaviors. Genetic mutations associated with ASD can either activate or inactivate the responsible proteins, affecting neuronal morphogenesis and contributing to the disorder's hallmark features. However, the molecular mechanisms driving these changes remain incompletely understood. Here, we report for the first time that the small GTP/GDP-binding protein Arf6 and FE65, which act together with the genetically conserved engulfment and cell motility 2 (ELMO2) signalosome to control Rac1, underlie the excessive neuronal process elongation phenotype associated with the ASD-linked semaphorin-5A (Sema5A) Arg676-to-Cys protein (p.Arg676Cys). Clustered regularly interspaced short palindromic repeats (CRISPR)/Cas13-mediated knockdown of Arf6 or FE65 reversed the excessively elongated processes in primary cortical neurons. Similar results were obtained in the N1E-115 cell line, a model capable of neuronal morphological differentiation. Moreover, expression of the ELMO2-binding domain of FE65 restored Rac1 activity required for process elongation,

recapitulating the effects seen in the knockdown experiments. These findings suggest that signaling through FE65 specifically couples Sema5A p.Arg676Cy to the ELMO2 signalosome molecule, driving excessively elongated processes with elevated Rac1 activity. One or more of these molecules may provide possible therapeutic targets for correcting the cellular phenotypes associated with the Sema5A p.Arg676Cys mutation in ASD.

Key words: Sema5A; autism spectrum disorder; Arf6; FE65; ELMO2; morphogenesis.

1. Introduction

Autism is a type of developmental disability, now more commonly referred to as autism spectrum disorder (ASD). ASD encompasses autism, pervasive developmental disorder, and Asperger syndrome [1-4]. Core symptoms of ASD include impaired social behavior and interpersonal communication, along with repetitive movements and strong attachment to specific objects [1-4]. Individuals with ASD are also often hypersensitive to light and sound stimuli, although some may instead exhibit hyposensitivity [1-4]. Therefore, ASD may be characterized as a neuro-integrative disorder of the sensory system involving the central nervous system (CNS) and, in some cases, the peripheral nervous system (PNS) [1-4]. ASD is believed to be caused by genetic and/or environmental factors. The majority of ASD cases (50%-90%) have familial or sporadic (i.e., *de novo*) gene mutations [5-8]. These mutations can cause a variety of amino acid changes, which may modulate the catalytic or binding activities of the encoded proteins, leading to either an increase or decrease in function [5-8]. These changes can also affect post-translational processing, protein stability, and subcellular localization [5, 6]. These gene mutations are thought to influence the cytomorphogenesis of neurons during neuritogenesis, and possibly during neurogenesis [5-8].

During CNS development, neuronal cells undergo continuous and dynamic cell morphogenesis [9, 10], including neurite growth and elongation, neurite navigation, and the formation of neuronal networks through synaptogenesis [11, 12]. However, the molecular mechanisms governing the different neuronal cell morphological differentiation stages have not yet been fully elucidated [11-14]. In neurological diseases, neuronal cell morphogenesis may be disrupted not only during early development but also at later and even very early stages [11-14]. The transmembrane protein semaphorin-5A (Sema5A) functions as an axon guidance cue in response to neuronal growth cone elongation and navigation [15-18]. Sema5A is a bifunctional axon guidance signal that sometimes functions as a ligand and sometimes as a receptor [19, 20]. Importantly, mutations in the *sema5a* gene are well known to be associated with ASD and are occasionally responsible for intellectual disability (ID), which is a neurodevelopmental disorder characterized by below-average intellectual functioning and impairments in conceptual and social communication [21-24]. Mutations in the *sema5a* gene are also associated with epilepsy [25, 26]. These abnormalities are believed to be directly related to the ability to form connections between different neuronal cells and/or to elongate neuronal processes necessary for connectivity in certain brain regions [27, 28].

We previously reported that an ASD-associated Sema5A Arg676-to-Cys (p.Arg676Cys) mutated protein induces excessive neuronal processes through a signalosome composed of the genetically conserved engulfment and cell motility 2 (ELMO2, also known as the CED-12 ortholog) and dedicator of cytokinesis 5 (DOCK5, also known as the CED-5 ortholog) as the Rac1 activator [29, 30]. Here, we describe that Sema5A p.Arg676Cys triggers intracellular signaling through the small GTP/GDP-binding protein Arf6 [31-34], leading to excessive axonal outgrowth in both cortical neuronal cells [35, 36] and the neuronal model cell line N1E-115 [37, 38]. Using clustered regularly interspaced short palindromic repeats (CRISPR)/Cas13 technology [39, 40], knockdown of FE65 (also known as amyloid beta precursor protein [APP] binding family B member 1 [APBB1]) [41-46], which acts upstream of the ELMO2 and DOCK5 signalosome controlling Rac1 as a central regulator of cytoskeletal changes and cell morphogenesis [47-50], specifically rescued both excessive process elongation and increased Rac1 activity induced by Sema5 p.Arg676Cys. Moreover, expression of the binding domain between FE65 and ELMO2 in cells decreased Rac1 activity and reversed excessive elongation. These findings indicate that signaling through FE65 specifically acts downstream of Sema5A p.Arg676Cy

and provide insight into potential drug-target molecule(s) for Sema5A-related ASD, at least at the molecular and cellular levels.

2. Materials and methods

2.1. Key antibodies and plasmids

Key materials used in this study are listed in Table 1.

2.2. Cell line culture and induction of differentiation

The mouse neuronal N1E-115 cell line (JCRB, Osaka, Japan) was cultured on cell culture dishes (Nunc brand, Thermo Fisher Scientific, Waltham, MA, USA) in high-glucose Dulbecco's modified Eagle medium (DMEM; Nacalai Tesque, Kyoto, Japan; Fujifilm Wako Chemicals, Tokyo, Japan) containing 10% heat-inactivated fetal bovine serum (FBS) (Gibco brand, Thermo Fisher Scientific) and penicillin-streptomycin solution (Nacalai Tesque) in 5% CO_2 at 37°C [37, 38]. Cells stably harboring the wild type *sema5a* gene (indicated as WT in the figures) or the gene with the p.Arg676Cys mutation (indicated as R676C in the figures) were selected as clones in the presence of the antibiotic G418 (0.5 mg/ml, Nacalai Tesque) for 2 weeks, in accordance with the manufacturer's instructions [29, 30]. These cells were maintained in culture without cryopreservation.

To induce differentiation, cells were cultured in DMEM and 1% FBS containing penicillin-streptomycin solution in 5% CO_2 at 37°C for several days, unless otherwise indicated. Cells with processes longer than one cell body were considered the longest process-bearing, differentiated cells (i.e., differentiated cells) [37, 38]. The length of the longest processes following induction of differentiation was measured in a blinded manner using Image J software (ver. Java 8, downloaded from https://imagej.nih.gov/). Under these conditions, the percentage of attached cells incorporating trypan blue (Nacalai Tesque) was estimated to be less than 5% in each experiment.

2.3. Primary cell culture and axon elongation

Animals were handled in accordance with the ARRIVE guidelines (https://arriveguidelines.org/), and all studies were conducted according to committee-approved protocols as described in the Ethics statement section. Mice were euthanized by chemical anesthesia using an intraperitoneal injection of a mixture of 0.3 mg/kg medetomidine, 4 mg/kg midazolam, and 5 mg/kg butorphanol. Primary cortical neuronal cells were isolated from the cerebrum of C57BL/6JJcl mice (Clea Japan, Inc., Tokyo, Japan) at embryonic days 16 to 17 and cultured as previously described [35, 36]. Following incubation with 100 units/ml papain (Worthington Biochemical, Lakewood, NJ, USA)

in Leibovitz's L-15 medium (Fujifilm Wako Chemicals) at 37°C for 15 min, cells were gently dissociated by pipetting. The dissociated cells were then plated at 3 to 5 × 10^5/cm^2 on polylysine-coated cell culture dishes (Nacalai Tesque). The culture medium consisted of Neurobasal medium supplemented with 2% B27 (Thermo Fisher Scientific), 1% GlutaMAX (Thermo Fisher Scientific), and 0.1 mg/ml gentamicin solution (Thermo Fisher Scientific). Cells were maintained in 5% CO_2 at 37°C. The medium was replaced with fresh medium 1 day after isolation; subsequently, half of the medium was replaced every 2 to 3 days. After maintaining the neurons for 7 to 14 days, cultured cortical neuronal cells were detached using 0.05% trypsin solution containing 0.53 mM EDTA (Thermo Fisher Scientific) and stored in liquid nitrogen until use.

To initiate experiments for observing process elongation, cells were reattached to cell culture dishes and processes were allowed to elongate for several days. A cell with a single axonal process longer than two cell body lengths was considered to be axonal process-bearing [35, 36]. The length of longest processes (axons) was measured in a blinded manner using Image J software. Under these conditions, the percentage of attached cells incorporating trypan blue was estimated to be less than 5% in each experiment.

2.4. Introduction of knocking down or protein-expressing plasmids

Cells and stable clones were transfected with or without the respective plasmids (either a mammalian expression plasmid encoding Cas13 for RNA knockdown [Addgene, Watertown, MA, USA] and the corresponding gRNAs inserted into a Pol III–type transcription plasmid [pSIN-mU6, Takara Bio, Kyoto, Japan] or mammalian expression plasmid based on pcDNA3.1 (+) or pCMV5) using the ScreenFect A transfection kit (Fujifilm Wako Chemicals). Transfections were performed in serum- and antibiotics-free high-glucose DMEM in accordance with the manufacturer's instructions.

Serum was added to the medium 4 hours post-transfection and the medium replaced at 24 hours post-transfection. Cells were then allowed to differentiate for 0 or 48 hours, depending on the experimental requirement for cell biological or biochemical studies, unless otherwise indicated. Under these conditions, the percentage of attached cells incorporating trypan blue was estimated to be less than 5% in each experiment.

2.5. Polyacrylamide gel electrophoresis and immunoblotting

Cells were lysed in lysis buffer (50 mM HEPES-NaOH, pH 7.5, 150 mM NaCl, 5 mM $MgCl_2$, 1 mM dithiothreitol [DTT], 1 mM

phenylmethane sulfonylfluoride [PMSF], 0.02 mM leupeptin, 1 mM EDTA, 1 mM Na_3VO_4, 10 mM NaF, and 0.5% NP-40). For standard denaturing conditions, centrifugally collected cell supernatants were denatured in sample buffer (Fujifilm Wako Chemicals). The samples were separated on a sodium dodecylsulfate polyacrylamide (SDS-PAGE) gel (Nacalai Tesque). Electrophoretically separated proteins were transferred to a polyvinylidene fluoride (PVDF) membrane (Fujifilm Wako Chemicals), blocked with Blocking One (Nacalai Tesque), and immunoblotted using primary antibodies, followed by peroxidase enzyme-conjugated secondary antibodies. Peroxidase-reactive bands were detected using X-ray film (Fujifilm, Tokyo, Japan) or TMB solution (Nacalai Tesque) and captured using a CanoScan LiDE4000 and CanoScan software (ver. 2024, Canon, Tokyo, Japan). The blots shown in the figures are representative of three independent experiments. In some experiments, immunoreactive bands were quantified relative to control bands using Image J software.

2.6. Assay for GTP-bound Rac1 or Cdc42

Cells were lysed in ice-cold G-LISA cell lysis buffer (G-LISA GTPase kit, Cytoskeleton, Inc., Denver, CO, USA). Briefly, centrifugally collected cell supernatants (equal sample volumes) were added to the reconstituted plate with affinity capture wells, which had

been removed from the plate holders. The wells were immediately placed on a cold orbital microplate shaker (400 rpm) in a low-temperature room and incubated with the supernatants and buffer controls to measure blank values for exactly 30 min. After incubation, the supernatants and controls were removed, and the wells were washed twice with G-LISA wash buffer.

At room temperature, G-LISA antigen-presenting buffer was added to each well, incubated at room temperature for exactly 2 min, and then washed three times with wash buffer. After the diluted primary antibody was added to each well, the plate was placed on an orbital microplate shaker at room temperature for 45 min. Next, the mixtures containing the primary antibody were removed, and the wells were washed twice with wash buffer.

Next, the wells were incubated with a peroxidase enzyme-conjugated secondary antibody, plated on a shaker at room temperature for 45 min, followed by three washes with wash buffer. Finally, the wells were incubated with the mixed HRP detection solution at room temperature for exactly 20 min, then treated with the HRP stop solution. Absorbance was measured at 490 nm using an MPR-A100, microplate spectrophotometer (AS ONE Co., Osaka, Japan). Blank values from each of the three experiments were subtracted, and results were quantified as G-LISA values.

After the assay, the plates were washed with a buffer containing 0.5 M NaCl and 0.5 M EDTA, rinsed with Dulbecco's phosphate-buffered saline, and stored at 4°C until use.

2.7. Fluorescent images

Cells on coverslips were fixed with 4% paraformaldehyde (Nacalai Tesque) or 100% cold methanol (Nacalai Tesque) and blocked with Blocking One. Slides were incubated with primary antibodies preloaded with fluorescent dye-conjugated secondary antibodies if necessary. Coverslips were mounted using the Vectashield kit with 4',6-diamidino-2-phenylindole (DAPI) (Vector Laboratories, Burlingame, CA, USA). The fluorescent images were collected, merged, and analyzed using an FV3000 microscope system equipped with a Fluoview laser-scanning apparatus and Fluoview software ver. 5 (both from Olympus, Tokyo, Japan), or a DMI4000B microscope system with AF6000 software ver. 2 (Leica, Wetzlar, Germany). The images in the figures are representative of several images and were analyzed using Image J software.

2.8. Statistical analyses

Values are presented as means ± standard deviation (SD) of independent experiments. Intergroup comparisons were performed

using the unpaired Student's *t*-test in Excel (ver. 2021, Microsoft, Redmond, WA, USA). One-way analysis of variance (ANOVA) was followed by the Tukey honest significant difference (HSD) test, using StatPlus Excel plug-in software (ver. 2021, Alexandria, VA, USA) when multiple comparisons were necessary. Differences were considered statistically significant when $p < 0.05$.

2.9. Ethics statement

All animal experiments were conducted in accordance with the protocol reviewed and approved by the Tokyo University of Pharmacy and Life Sciences Animal Care and Use Committee (Approval No. L24-20). Gene experiments were conducted according to the protocol reviewed and approved by the Tokyo University of Pharmacy and Life Sciences Gene Committee (Approval No. LSR3-01).

3. Results

3.1. Knockdown of Arf6 decreases mutated Sema5A-induced phenotypes

First, to investigate whether Arf6 is involved in the regulation of Sema5A p.Arg676Cys-mediated excessive process elongation (Figure S1, A and B, and Figure S2) [29, 30], we transfected N1E-115 cells stably harboring Sema5A p.Arg676Cys with plasmids encoding

either a control guide RNA (gRNA) or a gRNA targeting Arf6, together with Cas13 [39, 40]. At day 2 following the induction of differentiation, knockdown of Arf6 (Figure S3A) led to reduced process elongation compared with cells transfected with the control gRNA. In contrast, at day 0, neither control nor Arf6 knockdown had an apparent effect (Figure 1, A and B; Figure S4A). Similar results were observed in primary cortical neurons transfected with Sema5A p.Arg676Cys (Figure S5, A and B; Figure S6; Figure S7, A and B), suggesting that Arf6 is needed for neuronal process elongation in cells harboring Sema5A p.Arg676Cys. Notably, Arf6 knockdown affected Tau-positive axonal length.

Next, we examined whether knockdown of Arf6 affects neuronal differentiation marker expression. Despite the lack of any apparent effect from control or Arf6 knockdown at day 0 following the induction of differentiation (Figure 1, C and D), knockdown of Arf6 in cells harboring Sema5A p.Arg676Cys specifically decreased the expression levels of the neuronal differentiation markers 43 kDa nervous system specific, growth-associated protein (GAP43) and neuronal tubulin at day 2 following the induction of differentiation (Figure 1, E and F), indicating that Arf6 underlies Sema5A p.Arg676Cys-mediated excessive process elongation. In contrast,

expression levels of the internal control protein, actin, were comparable in Arf6- and control-knocked down cells.

3.2. Knockdown of FE65 decreases mutated Sema5A-induced phenotypes

We explored whether FE65, an adaptor protein coupling Arf6 to ELMO2 [41-46], is also involved in the regulation of Sema5A p.Arg676Cys-mediated excessive process elongation. Transfection of a plasmid encoding a gRNA for FE65 together with Cas13 (Figure S3B) into cells harboring Sema5A p.Arg676Cys led to decreased process elongation following the induction of differentiation (Figure 2, A and B; Figure S4B). These results were consistent with findings of decreased levels of neuronal differentiation marker protein expression (Figure 2, C and D), suggesting that FE65 mediates Sema5A p.Arg676Cys-induced excessive elongation. Similar cellular phenotypes were observed in primary cortical neurons transfected with Sema5A p.Arg676Cys (Figure S5, A and B; Figure S6; Figure S7, A and B).

3.3. Fe65-binding domain decreases mutated Sema5A-induced phenotypes

To examine whether the interaction of Arf6 and FE65 contributes to Sema5A p.Arg676Cys-mediated excessive process elongation, we transfected a plasmid encoding the FE65-binding domain (Figure S3C) into cells harboring Sema5A p.Arg676Cys. The FE65-binding domain decreased both Sema5A p.Arg676Cys-mediated excessive process elongation (Figure 3, A and B; Figure S4C) and levels of neuronal differentiation marker protein expression (Figure 3, C and D), indicating that the interaction of Arf6 and FE65 plays a role in Sema5A p.Arg676Cys-mediated excessive elongation. Similar results in cellular phenotypes were observed in primary cortical neurons transfected with Sema5A p.Arg676Cys (Figure S5, A and B; Figure S6; Figure S7, A and B).

3.4. Mutated Sema5A-induced activation of Rac1 is specifically mediated by FE65

Because Arf6 and FE65 act upstream of Rac1 as effector molecules of ELMO2 and DOCK5 in this signaling pathway, we measured the levels of Rac1·GTP using the G-LISA GTPase kit. After induction of differentiation, Rac1 was activated to similar levels in cells transfected with the control plasmid (mock) or cells harboring wild type Sema5A. Under these conditions, Rac1 activity was specifically inhibited by knockdown of Arf6 but not by knockdown of

FE65 or transfection of the FE65-binding domain (Figure 4A). This suggests that Arf6 is involved in Rac1 activation during normal process elongation, whereas FE65, one of the Arf6 effectors, is not involved. In contrast, Sema5A p.Arg676Cys-mediated activation of Rac1 was decreased by knockdown of Arf6 or FE65 or by transfection of the FE65-binding domain. Similarly, Sema5A p.Arg676Cys-mediated activation of Rac1 was decreased by knockdown of Arf6 or FE65 or by transfection of the FE65-binding domain in primary cortical neurons (Figure S8).

These results were consistent with the observation that, in parental cells (non-transfected cells), knockdown of Arf6, but not knockdown of FE65 or transfection of the FE65-binding domain, specifically inhibited the expression of neuronal marker proteins following the induction of differentiation (Figure S9, A-C). Similar phenomena in the case of Arf6 knockdown were observed in cells harboring wild type Sema5A either at the marker protein levels (Figure S10, A-C) or at the cell morphological levels (Figure S11, A-C; Figure S12, A-C), suggesting that signaling through FE65 specifically mediates effects of Sema5A p.Arg676Cys.

In contrast, in cells harboring wild type or mutated Sema5A, Cdc42 was activated after induction of differentiation, but the signal was independent of Arf6 and FE65 (Figure 4B).

3.5. Formation of an ELMO2 complex in cells is mediated by Arf6 and FE65

Finally, we investigated whether Arf6 and FE65 can control the formation of the genetically conserved signalosome containing ELMO2 and DOCK5 in cells. Knockdown of Arf6 or FE65 led to a decreased number of signalosomes labeled with red fluorescence protein (RFP)-tagged ELMO2 in the cell bodies of cells harboring Sema5A p.Arg676Cys (Figure S13, A-C). Similar results were obtained for processes and growth cones, although their numbers were much smaller than those in cell bodies.

Taken together, these findings suggest that a protein complex centered on ELMO2 and DOCK5 is involved in signaling that controls Sema5A p.Arg676Cys-mediated excessive process elongation.

4. Discussion

Genetic mutations in ASD patients affect neuronal morphology and function, as well as the relationships between excitatory and inhibitory neurons, neurons and glia, and neurons and immune cells in the brain [5-8]. Abnormal neuronal morphogenesis and developmental patterns may contribute to the formation of ASD as a neurodevelopmental disorder. The structure and function of the

responsible gene products are altered by amino acid substitutions, which may affect neuronal morphogenesis and morphology [5-8]. However, despite the relationship between ASD-associated amino acid mutations and cell morphology, it remains unclear which signaling units these mutations use to specifically induce abnormal neuronal morphological changes.

Many human genetic studies have shown that deletions in the short arm region of chromosome 5 are associated with phenotypic features such as ASD, infantile crying syndrome, ID, and microcephaly [21, 23]. Classical transcriptome analysis has also revealed that some autistic individuals exhibit low levels of several transcripts encoded in the short arm region of chromosome 5 [21]. This chromosomal deletion region includes *sema5a* and several other genes, some of which have been linked to infantile epilepsy [23]. Furthermore, mutations in Sema5A protein occur between the extracellular and intracellular regions, allowing for the formation of potential disulfide bonds in the extracellular region and possible reducing groups in the intracellular region, within the predicted topological domain structure [23]. Importantly, Sema5A has been shown to be critically associated with ASD, often accompanied by ID, depending on the individual patient, suggesting that Sema5A is indeed the causative gene product of ASD.

The activity of ASD-associated mutated Sema5A protein generally involves activation or inactivation compared with the wild type protein [23]. We have previously shown that Sema5A is activated by mutations at p.Arg676Cys or p.Ser951Cys, with p.Arg676Cys being particularly active through effective cell surface trafficking and/or secretion of Sema5A [29, 30]. Sema5A acts in an autocrine manner by interacting with an unknown receptor on the cell surface, suggesting its role as a ligand [17, 18], although Sema5A can be a bifunctional transmembrane protein that also acts as a receptor [51]. In both scenarios, the effects of mutated Sema5A are mediated by a genetically conserved signalosome that includes ELMO2 and DOCK5, resulting in excessive process elongation.

Here, we describe a mechanism in which FE65 specifically cooperates with ELMO2 and DOCK5 to activate Rac1 during the excessive process elongation induced by Sema5A p.Arg676Cy. FE65 is generally recognized as a scaffold protein that interacts with GDP-bound Arf6 [41-44], helping to recruit ELMO and DOCK molecules. It is thought that FE65 couples the signaling elicited by mutated Sema5A to ELMO2 and DOCK5. Arf6 is a multifunctional GTP/GDP-binding protein that is not only a regulator of intracellular vesicle transporting but is also involved in cytoskeletal rearrangement [52]. FE65 contains several protein-protein interaction domains, including

an N-terminal proline-rich sequence–binding WW domain and two C-terminal phosphotyrosine-binding (PTB) domains, and was originally identified as a non-enzymatic binding partner of APP [53]. FE65, often acting together with Arf6, mediates the assembly of multimolecular complexes [43], suggesting that FE65 could be the molecule in the ELMO2 and DOCK5 signalosome that activates Rac1 in the cellular pathological states observed in Sema5A p.Arg676Cys.

FE65 is known to be involved in a variety of neuronal developmental and functional events, ranging from neurogenesis to synaptogenesis, synaptic plasticity, learning, and memory [41, 42]. In particular, FE65 is likely to contribute to neuronal networks in later stages [41, 42]. Thus, dysfunction of FE65, acting together with disease-related molecules such as APP, is associated with the development of diseases such as dementia [41]. These functional changes in the structure and function of FE65 in health and disease may be reminiscent of the neuronal morphological changes observed in Sema5A p.Arg676Cys.

It remains unclear whether there is a specific signaling cassette connecting Sema5A p.Arg676Cys and FE65 in cells. The BioGRID$^{4.4}$ interactome database (see https://thebiogrid.org) identifies approximately 200 known and potential molecules that may interact with FE65. Among these, a group of Rab family GTP/GDP-

binding proteins are listed as potential FE65-interacting molecular candidates. Similar to the Arf family proteins, Rab proteins have roles in controlling intracellular vesicle trafficking by marking the inner surface of the membrane of each organelle in various types of cells [54]. It is possible that FE65, through binding to Arf6 and some Rab proteins, mediates Sema5A p.Arg676Cys-induced activation of Rac1 by ELMO2 and DOCK5 on the respective predicted organelles. Furthermore, FE65 can interact with the FE65 homolog FE65L1 (according to the BioGRID$^{4.4}$ database), and this potential interaction may extend its interactions with other small GTP/GDP-binding proteins [31, 34, 53].

Small GTP/GDP-binding proteins, including Arf6, plays a significant role in neuronal development [55, 56]. Arf6 contributes to Rac1 activation via a signaling complex comprising FE65, ELMO family proteins (e.g., ELMO2), and DOCK family proteins (e.g., DOCK5) [41-44]. This activation of Rac1 ultimately supports neurite outgrowth, neuronal network remodeling, and synapse formation [47-50]. It is hypothesized that small GTP/GDP-binding proteins including Arf6 affect axonal outgrowth and elongation through continuous and indirect interactions with Rho family small GTPases including Rac1 [41, 42, 56].

In the present study, we demonstrate that Arf6, FE65, and ELMO2 mediate the excessive process elongation induced by the ASD-associated Sema5A p.Arg676Cys variant in neuronal cells. It is well established that Arf6 recruits FE65 and its binding partners through interaction with its GDP-bound form [41–44]. Consistent with this mechanism, our findings complement previous reports showing that mutations in the guanine-nucleotide exchange factor IQ motif and Sec7 domain-containing protein 2 (IQSEC2) are implicated in ASD [56–60]. Together, these signaling pathways may contribute to ASD-related abnormalities in neuronal morphology. Moreover, IQSEC2-dependent activation of Arf6 [31–34] is likely to regulate a broad range of downstream targets, including organelle-associated proteins and lipid-modifying signaling enzymes (Figure S14). Further studies are needed to enhance our understanding of the detailed molecular mechanisms by which signaling around FE65 mediates mutated Sema5A-induced phenotypes, and to determine whether their inhibition can recover these phenotypes *ex vivo* and in genetically modified mice under ASD model conditions. These studies will help us elucidate the full scope of the unique signaling mechanisms involving genetically conserved ELMO2 and DOCK5, which act downstream of mutated Sema5A, at least at the molecular and cellular levels. Such studies could lead to the development of drug target-specific

treatments for diseases associated with Sema5A p.Arg676Cys and related disorders.

5. References

1. Bernier, R., Mao, A., Yen, J. Psychopathology, families, and culture: autism. Child Adolesc. Psychiatr. Clin. N. Am. 2010 19:855-867
2. Mazza, M., Pino, M. C., Mariano, M., Tempesta, D., Ferrana, M., Berardis, D. D., Masedu, F., Valenti, M. Affective and cognitive empathy in adolescents with autism spectrum disorder. Front. Hum. Neurosci. 2014 8:791
3. Arnett, A. B., Trinh, S., Bernier, R. A. The state of research on the genetics of autism spectrum disorder: methodological, clinical and conceptual progress. Curr. Opin. Psychol. 2019 27:1-5
4. Peterson, J. L., Earl, R., Fox, E. A., Ma, R., Haidar, G., Pepper, M., Berliner, L., Wallace, A., Bernier, R. Trauma and autism spectrum disorder: Review, proposed treatment adaptations and future directions. J. Child. Adolesc. Trauma 2019 12:529-547
5. Modabbernia, A., Velthorst, E., Reichenberg, A. Environmental risk factors for autism: an evidence-based review of systematic reviews and meta-analyses. Mol. Autism. 2017 8:13
6. Varghese, M., Keshav, N., Jacot-Descombes, S., Warda, T., Wicinski, B., Dickstein, D. L., Harony-Nicolas, H., De Rubeis, S., Drapeau, E., Buxbaum, J. D., Hof, P. R. Autism spectrum disorder: neuropathology and animal models. Acta Neuropathol. 2017 134:537-566

7. Genovese, A., Butler, M. G. Clinical assessment, genetics, and treatment approaches in autism spectrum disorder (ASD). Int. J. Mol. Sci. 2020 21:4726

8. Wang, L., Wang, B., Wu, C., Wang, J., Sun, M. Autism spectrum disorder: neurodevelopmental risk factors, biological mechanism, and precision therapy. Int. J. Mol. Sci. 2023 24:1819

9. Bray, D. Surface movements during the growth of single explanted neurons. Proc. Natl. Acad. Sci. USA. 1970 65:905-910

10. Rigby, M. J., Gomez, T. M., Puglielli, L. Glial cell-axonal growth cone interactions in neurodevelopment and regeneration. Front. Neurosci. 2020 14:203

11. Craig, A. M., Banker, G. Neuronal polarity. Annu. Rev. Neurosci. 1994 17:267-310

12. da Silva, J. S., C. G. Dotti. Breaking the neuronal sphere: regulation of the actin cytoskeleton in neuritogenesis. Nat. Rev. Neurosci. 2002 3:694-704

13. Arimura, N., K. Kaibuchi. Neuronal polarity: from extracellular signals to intracellular mechanisms. Nat. Rev. Neurosci. 2007 8:194-205

14. Park, H., Poo, M. M. Neurotrophin regulation of neural circuit development and function. Nat. Rev. Neurosci. 2013 14:7-23

15. Worzfeld, T., Offermanns, S. Semaphorins and plexins as therapeutic targets. Nat. Rev. Drug Discov. 2014 13:603-621.

16. Lin, L., Lesnick, T. G., Maraganore, D. M., Isacson, O. Axon guidance and synaptic maintenance: preclinical markers for neurodegenerative disease and therapeutics. Trends. Neurosci. 2009 32:142-149

17. Limoni, G., Niquille, M. Semaphorins and plexins in central nervous system patterning: the key to it all? Curr. Opin. Neurobiol. 2021 66:224-232

18. Zang, Y., Chaudhari, K., Bashaw, G. J. New insights into the molecular mechanisms of axon guidance receptor regulation and signaling. Curr. Top. Dev. Biol. 2021 142:147-196

19. Goldberg, J. L., Vargas, M. E., Wang, J. T., Mandemakers, W., Oster, S. F., Sretavan, D. W., Barres, B. A. An oligodendrocyte lineage-specific semaphorin, Sema5A, inhibits axon growth by retinal ganglion cells. J. Neurosci. 2004 24:4989-4999

20. Matsuoka, R. L., Chivatakarn, O., Badea, T. C., Samuels, I. S., Cahill, H., Katayama, K., Kumar, S. R., Suto, F., Chédotal, A., Peachey, N. S., Nathans, J., Yoshida, Y., Giger, R. J., Kolodkin, A. L. Class 5 transmembrane semaphorins control selective mammalian retinal lamination and function. Neuron. 2011 71:460-473

21. Melin, M., Carlsson, B., Anckarsater, H., Rastam, M., Betancur, C., Isaksson, A., Gillberg, C., Dahl, N. Constitutional downregulation of SEMA5A expression in autism. Neuropsychobiology 2006 54:64-69

22. Zhang, B., Willing, M., Grange, D. K., Shinawi, M., Manwaring, L., Vineyard, M., Kulkarni, S., Cottrell, C. E. Multigenerational autosomal dominant inheritance of 5p chromosomal deletions. Am. J. Med. Genet. A. 2016 170:583-593

23. Mosca-Boidron, A. L., Gueneau, L., Huguet, G., Goldenberg, A., Henry, C., Gigot, N., Pallesi-Pocachard, E., Falace, A., Duplomb, L., Thevenon, J., Duffourd, Y., St-Onge, J., Chambon, P., Rivière, J. B., Thauvin-Robinet, C., Callier, P., Marle, N., Payet, M., Ragon, C., Goubran Botros, H., Buratti, J., Calderari. S., Dumas, G., Delorme, R., Lagarde, N., Pinoit, J. M., Rosier, A., Masurel-Paulet, A., Cardoso, C., Mugneret, F., Saugier-Veber, P., Campion, D,, Faivre, L., Bourgeron, T. A *de novo* microdeletion of SEMA5A in a boy with autism spectrum disorder and intellectual disability. Eur. J. Hum Genet. 2016 24:838-843

24. Ito, H., Morishita, R., Nagata, K. I. Autism spectrum disorder-associated genes and the development of dentate granule cells. Med. Mol. Morphol. 2017 50:123-129

25. Depienne, C., Magnin, E., Bouteiller, D., Stevanin, G., Saint-Martin, C., Vidailhet, M., Apartis, E., Hirsch, E., LeGuern, E., Labauge, P., Rumbach, L. Familial cortical myoclonic tremor with epilepsy: the third locus (FCMTE3) maps to 5p. Neurology 2010 74:2000-2003

26. Wang, Q., Liu, Z., Lin, Z., Zhang, R., Lu, Y., Su, W., Li, F., Xu, X., Tu, M., Lou, Y., Zhao, J., Zheng, X. *De novo* germline mutations in SEMA5A associated with infantile spasms. Front. Genet. 2019 10:605

27. Gunn, R. K., Huentelman, M. J., Brown, R. E. Are Sema5a mutant mice a good model of autism? A behavioral analysis of sensory systems, emotionality and cognition. Behav. Brain Res. 2011 225:142-150

28. Duan, Y., Wang, S. H., Song, J., Mironova, Y., Ming, G. L., Kolodkin, A. L., Giger, R. J. Semaphorin 5A inhibits synaptogenesis in early postnatal- and adult-born hippocampal dentate granule cells. eLife. 2014 3:e04390

29. Okabe, M., Miyamoto, Y., Ikoma, Y., Takahashi, M., Shirai, R., Kukimoto-Niino, M., Shirouzu, M., Yamauchi, J. RhoG-binding domain of Elmo1 ameliorates excessive process elongation induced by autism spectrum disorder-associated Sema5A. Pathophysiology 2023 30:548-566

30. Okabe, M., Sato, T., Takahashi, M., Honjo, A., Okawa, M., Ishida, M., Kukimoto-Niino, M., Shirouzu, M., Miyamoto, Y., Yamauchi, J. Autism spectrum disorder- and/or intellectual disability-associated semaphorin-5A exploits the mechanism by which Dock5 signalosome molecules control cell shape. Curr. Issues Mol. Biol. 2024 46:3092-3107

31. Donaldson, J. G., Jackson, C. L. ARF family G proteins and their regulators: roles in membrane transport, development and disease. Nat. Rev. Mol. Cell Biol. 2011 12:362-375

32. Ito, A., Fukaya, M., Okamoto, H., Sakagami, H. Physiological and pathological roles of the cytohesin family in neurons. Int. J. Mol. Sci. 2022 23:5087

33. Sun, D., Guo, Y., Tang, P., Li, H., Chen, L. Arf6 as a therapeutic target: structure, mechanism, and inhibitors. Acta. Pharm. Sin. B 2023 13:4089-4104

34. Torii, T., Miyamoto, Y., Yamauchi, J. Myelination by signaling through Arf guanine nucleotide exchange factor. J. Neurochem. 2024 168:2201-2213

35. Numakawa, T., Yokomaku, D., Kiyosue, K., Adachi, N., Matsumoto, T., Numakawa, Y., Taguchi, T., Hatanaka, H., Yamada, M. Basic fibroblast growth factor evokes a rapid glutamate release through

activation of the MAPK pathway in cultured cortical neurons. J. Biol. Chem. 2002 277:28861-28869

36. Hwang, S., Lee, S. E., Ahn, S. G., Lee, G. H. Psoralidin stimulates expression of immediate-early genes and synapse development in primary cortical neurons. Neurochem. Res. 2018 43:2460-2472

37. Amano, T., Richelson, E., Nirenberg, M. Neurotransmitter synthesis by neuroblastoma clones. Proc. Natl. Acad. Sci. USA 1972 69:258-263

38. Hirose, M., Ishizaki, T., Watanabe, N., Uehata, M., Kranenburg, O., Moolenaar, W. H., Matsumura, F., Maekawa, M., Bito, H., Narumiya, S. Molecular dissection of the Rho-associated protein kinase (p160ROCK)-regulated neurite remodeling in neuroblastoma N1E-115 cells. J. Cell Biol. 1998 141:1625-1636

39. Konermann, S., Lotfy, P., Brideau, N. J., Oki, J., Shokhirev, M. N., Hsu, P. D. Transcriptome engineering with RNA-targeting type VI-D CRISPR effectors. Cell 2018 173:665-676

40. Yan, W. X., Chong, S., Zhang, H., Makarova, K. S., Koonin, E. V., Cheng, D. R., Scott, D. A. Cas13d Is a compact RNA-targeting type VI CRISPR effector positively modulated by a WYL-domain-containing accessory protein. Mol. Cell 2018 70:327-339

41. Chow, W. N., Cheung, H. N., Li, W., Lau, K. F. Fe65: roles beyond amyloid precursor protein processing. Cell Mol. Biol. Lett. 2015 20:66-87

42. Augustin, V., Kins, S. Fe65: a scaffolding protein of actin regulators. Cells 2021 10:1599

43. Cheung, H. N., Dunbar, C., Mórotz, G. M., Cheng, W. H., Chan, H. Y., Miller, C. C., Lau, K. F. FE65 interacts with ADP-ribosylation factor 6 to promote neurite outgrowth. FASEB J. 2014 28:337-349

44. Chan, W. W. R., Li, W., Chang, R. C. C., Lau, K. F. ARF6-Rac1 signaling-mediated neurite outgrowth is potentiated by the neuronal adaptor FE65 through orchestrating ARF6 and ELMO1. FASEB J. 2020 34:16397-16413

45. Zhai, Y., Chan, W. W. R., Li, W., Lau, K. F. ARNO is recruited by the neuronal adaptor FE65 to potentiate ARF6-mediated neurite outgrowth. Open Biol. 2022 12:220071

46. Chau, D. D., Li, W., Chan, W. W. R., Sun, J. K., Zhai, Y., Chow, H. M., Lau, K. F. Insulin stimulates atypical protein kinase C-mediated phosphorylation of the neuronal adaptor FE65 to potentiate neurite outgrowth by activating ARF6-Rac1 signaling. FASEB J. 2022 36:e22594

47. Reddien, P. W., Horvitz, H. R. The engulfment process of programmed cell death in *Caenorhabditis elegans*. Annu. Rev. Cell Dev. Biol. 2004 20:193-221

48. Citi, S., Guerrera, D., Spadaro, D., Shah, J. Epithelial junctions and Rho family GTPases: the zonular signalosome. Small GTPases 2014 5:1-15

49. Kukimoto-Niino, M., Ihara, K., Murayama, K., Shirouzu, M. Structural insights into the small GTPase specificity of the DOCK guanine nucleotide exchange factors. Curr. Opin. Struct. Biol. 2021 71:249-258

50. Kukimoto-Niino, M., Katsura, K., Ishizuka-Katsura, Y., Mishima-Tsumagari, C., Yonemochi, M., Inoue, M., Nakagawa, R., Kaushik, R., Zhang, K. Y. J., Shirouzu, M. RhoG facilitates a conformational transition in the guanine nucleotide exchange factor complex DOCK5/ELMO1 to an open state. J. Biol. Chem. 2024 300:107459

51. Nagy, G. N., Zhao, X. F., Karlsson, R., Wang, K., Duman, R., Harlos, K., El Omari, K., Wagner, A., Clausen, H., Miller, R. L., Giger, R. J., Jones, E. Y. Structure and function of Semaphorin-5A glycosaminoglycan interactions. Nat. Commun. 2024 15:2723

52. Hashimoto, A., Hashimoto, S. ADP-ribosylation factor 6 pathway acts as a key executor of mesenchymal tumor plasticity. Int. J. Mol. Sci. 2023 24:14934

53. Chau, D. D., Ng, L. L., Zhai, Y., Lau, K. F. Amyloid precursor protein and its interacting proteins in neurodevelopment. Biochem. Soc. Trans. 2023 51:1647-1659

54. Lu, S. L., Noda, T. The emerging role of Rab proteins in osteoclast organelle biogenesis and function. Biochem. Soc. Trans. 2024 52:2469-2475

55. Jaworski, J. ARF6 in the nervous system. Eur. J. Cell Biol. 2007 86:513-524

56. Ito, A., Fukaya, M., Okamoto, H., Sakagami, H. Physiological and pathological roles of the cytohesin family in neurons. Int. J. Mol. Sci. 2022 23:5087

57. Rogers, E. J., Jada, R., Schragenheim-Rozales, K., Sah, M., Cortes, M., Florence, M., Levy, N. S., Moss, R., Walikonis, R. S., Palty, R., Shalgi, R., Lichtman, D., Kavushansky, A., Gerges, N. Z., Kahn, I., Umanah, G. K. E., Levy, A. P. An IQSEC2 mutation associated with intellectual disability and autism results in decreased surface AMPA receptors. Front. Mol. Neurosci. 2019 12:43

58. Levy, N. S., Umanah, G. K. E., Rogers, E. J., Jada, R., Lache, O., Levy, A. P. IQSEC2-associated intellectual disability and autism. Int. J. Mol. Sci. 2019 20:3038

59. Levy, N. S., Borisov, V., Lache, O., Levy, A. P. Molecular insights into IQSEC2 disease. Int. J. Mol. Sci. 2023 24:4984

60. Shokhen, M., Walikonis, R., Uversky, V. N., Allbeck, A., Zezelic, C., Feldman, D., Levy, N. S., Levy, A. P. Molecular modeling of ARF6 dysregulation caused by mutations in IQSEC2. J. Biomol. Struct. Dyn. 2024 42:1268-1279

Acknowledgments

We thank Drs. Takako Morimoto and Yoichi Seki (School of Life Sciences, Tokyo University of Pharmacy and Life Sciences) for the insightful comments they provided throughout this study.

Funding sources

This work was supported by the Core Research for Evolutional Science and Technology (CREST) program of the Japan Science and Technology Agency (JST). Additional support was provided by Grants-in-Aid for Scientific Research from the Japanese Ministry of Education, Culture, Sports, Science and Technology (MEXT) and Grants-in-Aid for Medical Scientific Research from the Japanese Ministry of Health, Labour and Welfare (MHLW). We also received funding from the Daiichi Sankyo Science Foundation, Japan Foundation for Pediatric Research, Mishima Kaiun Memorial Foundation, Mitsubishi Tanabe Science Foundation, Otsuka Science Foundation, and Takeda Science Foundation.

Author contributions

Junji Yamauchi designed and organized the study. Yuki Miyamoto and Junji Yamauchi wrote and edited the manuscript. Mikito Takahashi and Hideji Yako performed experiments. Mikito Takahashi and Hideji Yako performed statistical analyses. Hideji Yako, Mutsuko Kukimoto-

Niino, and Mikako Shirouzu evaluated experimental and statistical data.

Competing interests

The authors declare no conflict of interest.

Data Availabilities

The datasets used and/or analyzed for the current study are available from the corresponding author upon reasonable request.

List of supplemental figures

This manuscript contains supplemental materials including computer-saved full-size gel images.

Figure and table legends

Figure 1. CRISPR/Cas13-mediated knockdown of Arf6 recovers mutated Sema5A-induced excessive process elongation. (A, B) N1E-115 cells stably harboring Sema5A p.Arg676Cys (R676C) were transfected with plasmids encoding gRNA for Arf6 (gArf6) or luciferase (gControl) together with Cas13 and cultured for 0 or 2 days following the induction of differentiation. Representative images are shown. Cells with processes with a body length of more than one cell were counted as exhibiting neurite-like process elongation and are depicted statistically (** $p < 0.01$; n = 10 fields). Lysates from cells at day 0 (C, D) or day 2 (E, F) following the induction of differentiation were immunoblotted using antibodies against neuronal differentiation marker proteins GAP43 and b3 tubulin, Arf6, or an internal control marker protein actin. Immunoreactive band values are calculated by dividing the band intensity of the marker protein by the band intensity of the actin protein and expressed statistically (* $p < 0.05$, ** $p < 0.01$; n = 3 blots).

Figure 2. CRISPR/Cas13-mediated knockdown of FE65 recovers mutated Sema5A-induced excessive process elongation. (A, B) Cells stably harboring Sema5A p.Arg676Cys (R676C) were transfected with plasmids encoding gRNA for FE65 (gFe65) or

luciferase (gControl) together with Cas13 and cultured for 0 or 2 days following the induction of differentiation. Representative images are shown. Cells with processes are depicted statistically (** $p < 0.01$; n = 10 fields). (C, D) Cell lysates following the induction of differentiation were immunoblotted with antibodies against neuronal differentiation marker proteins GAP43 and b3 tubulin, FE65, or an internal control marker protein actin. Immunoreactive band values are calculated by dividing the band intensity of the marker protein by the band intensity of the actin protein and expressed statistically (* $p < 0.05$, ** $p < 0.01$; n = 3 blots).

Figure 3. Transfection of the FE65-binding domain recovers mutated Sema5A-induced excessive process elongation. (A, B) Cells stably harboring Sema5A p.Arg676Cys (R676C) were transfected with plasmids encoding the FE65-binding domain (FBD) tagged with GFP or its vector (control), and cultured for 0 or 2 days following the induction of differentiation. Representative images are shown. Cells with processes are depicted statistically (** $p < 0.01$; n = 10 fields). (C, D) Cell lysates following the induction of differentiation were immunoblotted with antibodies against neuronal differentiation marker proteins GAP43 and b3 tubulin, GFP, or an internal control marker protein actin. Immunoreactive band values are

calculated by dividing the band intensity of the marker protein by the band intensity of the actin protein and expressed statistically (* $p < 0.05$; n = 3 blots).

Figure 4. Knockdown of Arf6 or FE65 or transfection of the FE65-binding domain recovers mutated Sema5A-induced excessive Rac1 activation. (A, B) Cells stably harboring wild type Sema5A (WT) or Sema5A p.Arg676Cys (R676C) were transfected with plasmids encoding gRNA for Arf6 (gArf6) or FE65 (gFe65) or luciferase (gControl) plus Cas13 or FE65-binding domain (FBD) or its empty vector (vector) and cultured for 2 days with (+) or without (-) differentiation induction. Cell lysates were analyzed using a G-LISA GTPase kit to assay the amounts of GTP-bound Rac1 or Cdc42 (** $p < 0.01$; n = 3).

Table 1. Key materials used in this study.

Figure 1

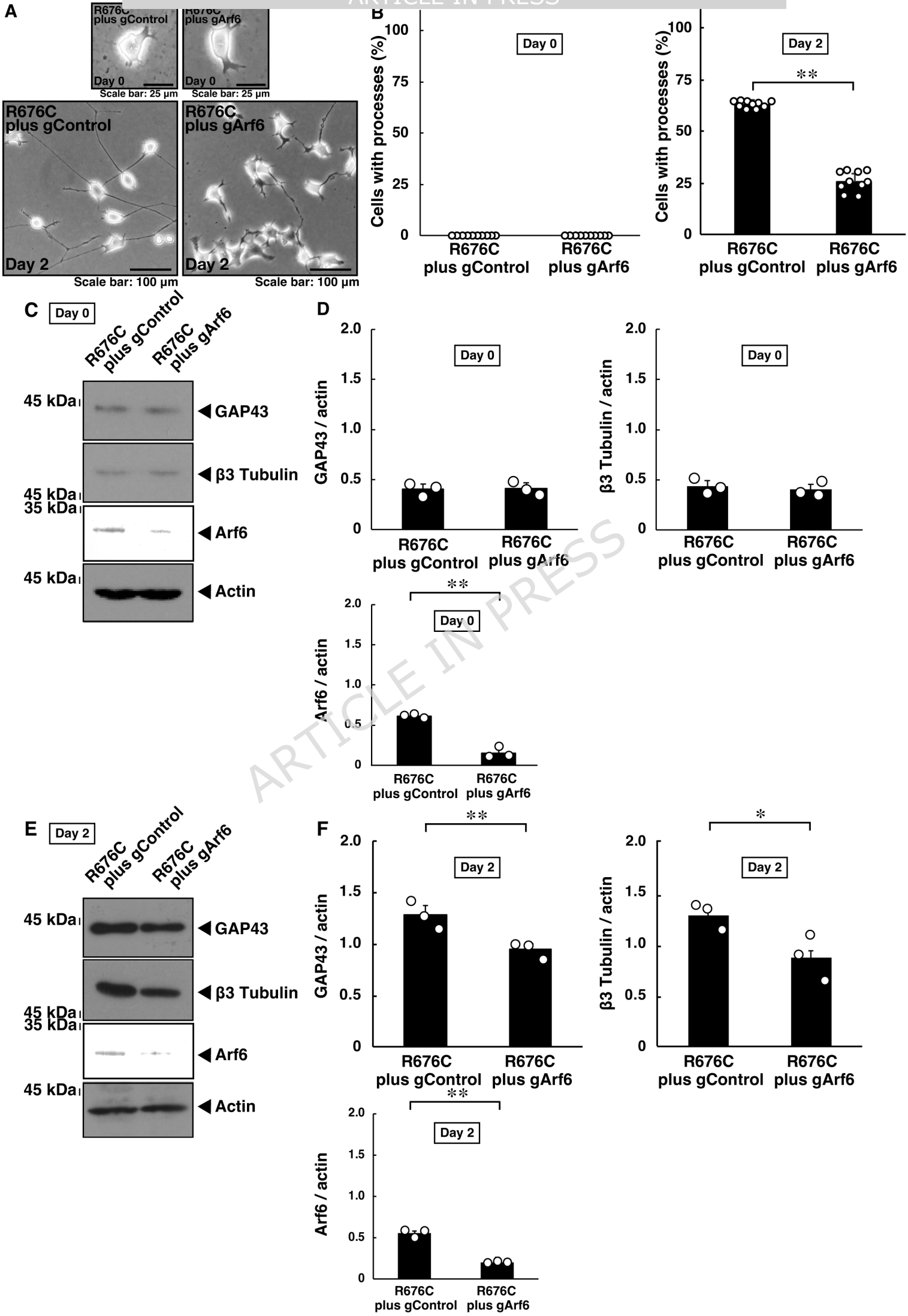

Figure 2

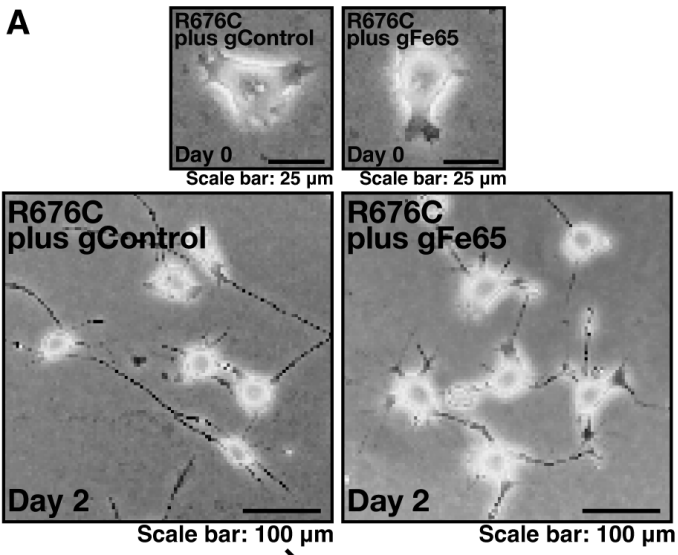

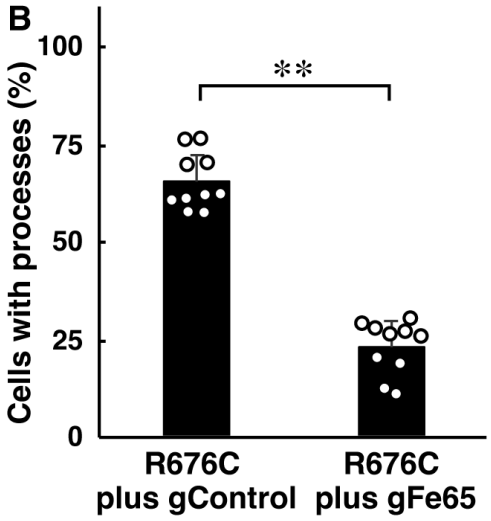

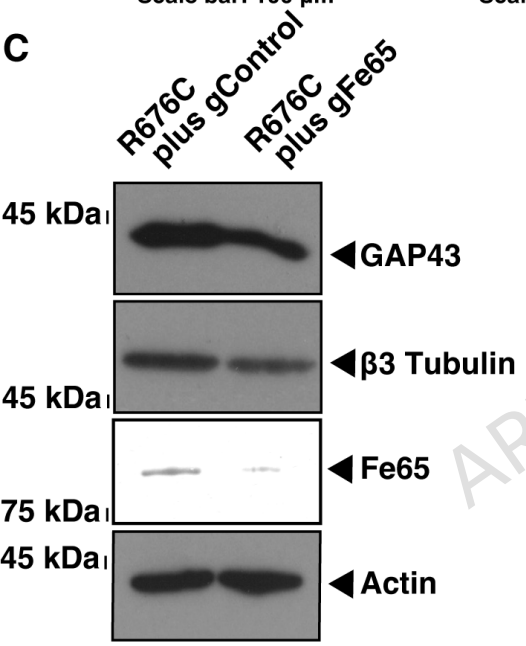

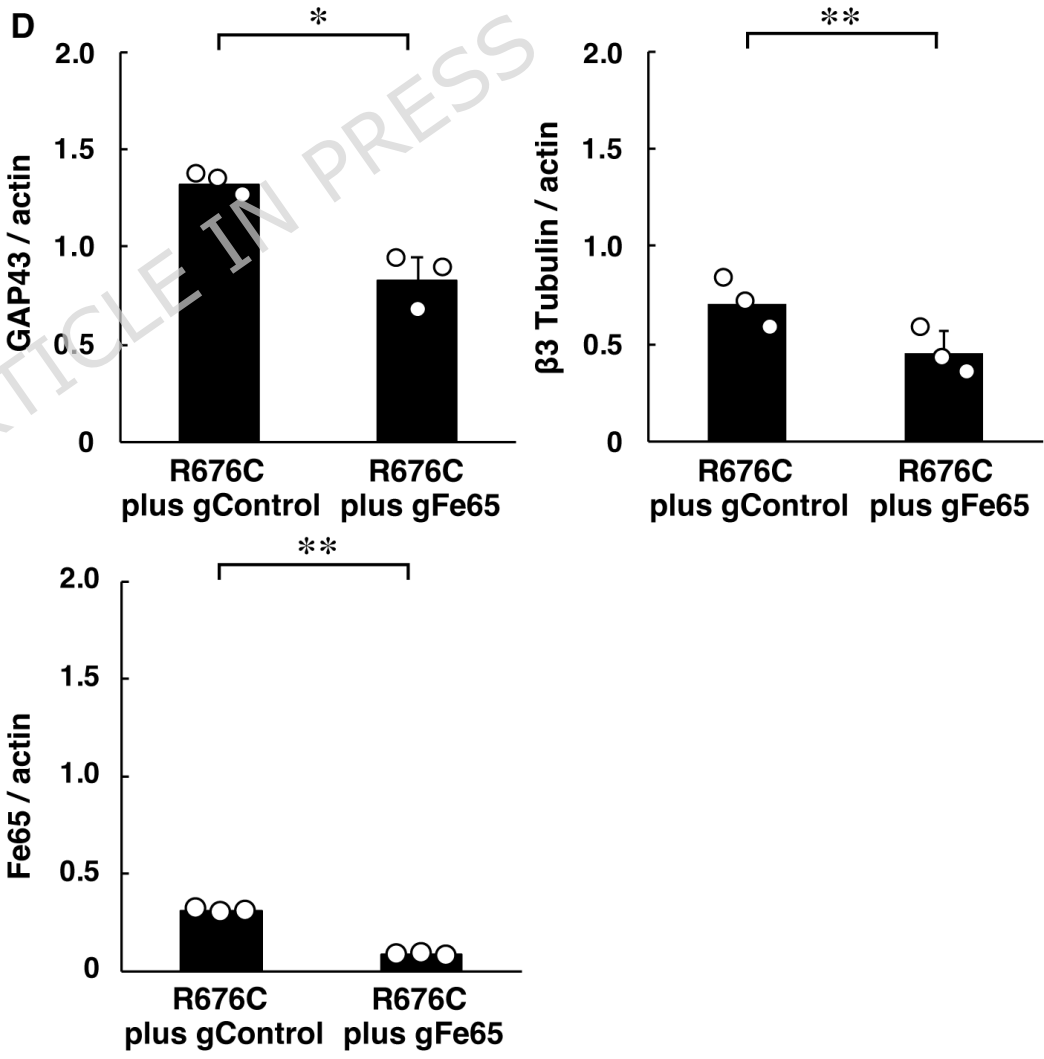

Figure 3

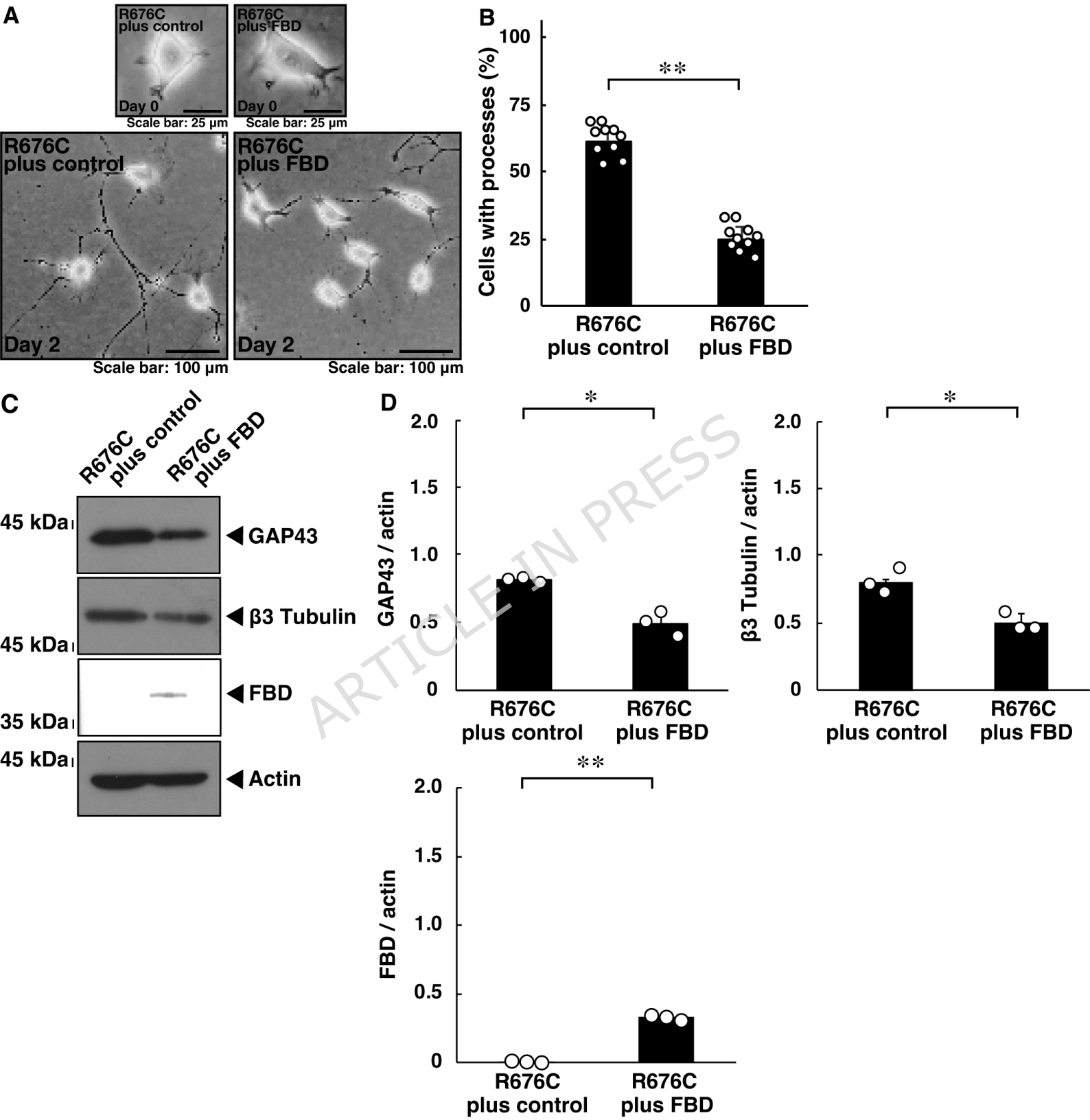

Figure 4

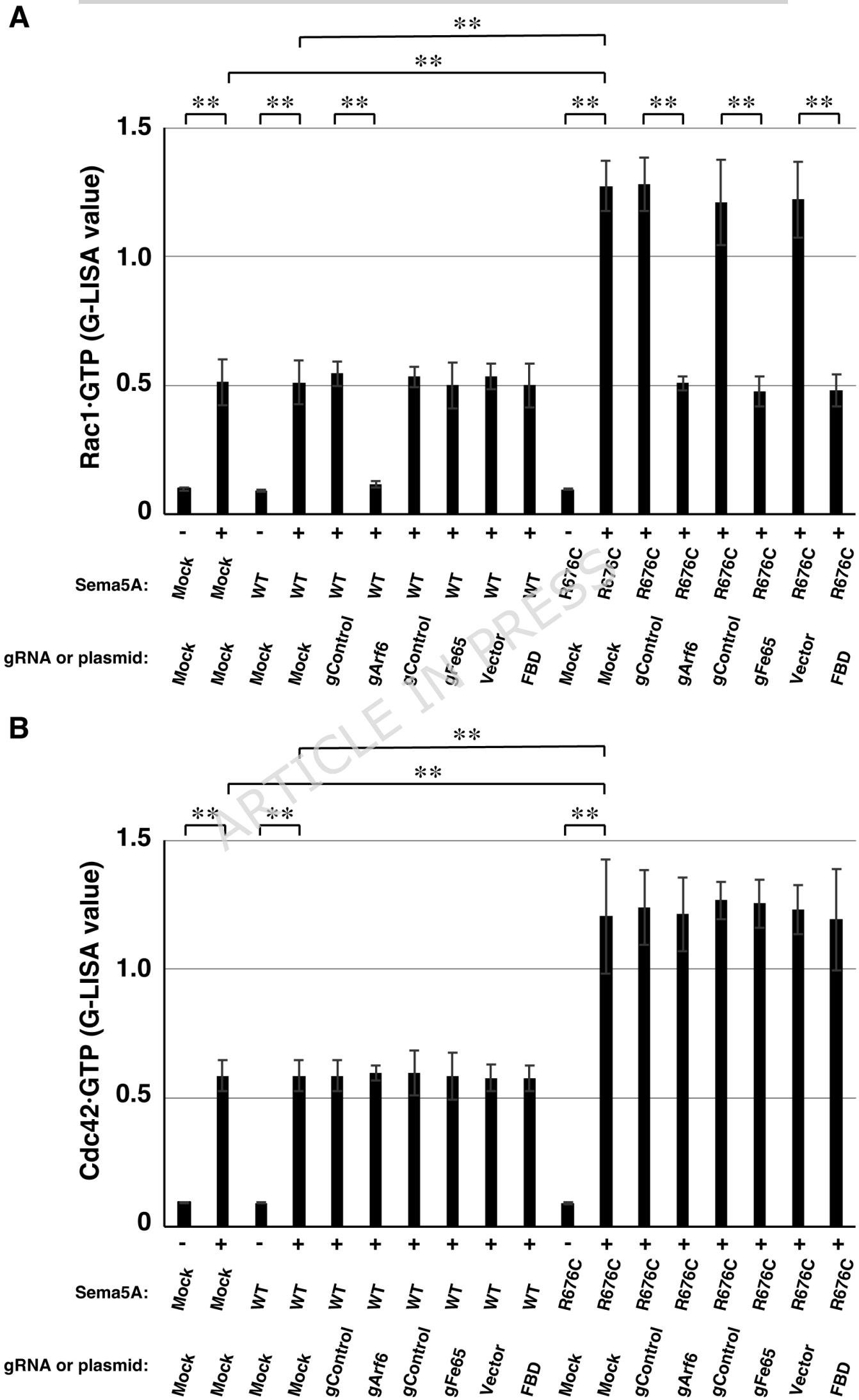

Reagents or materials	Companies or sources	Cat. Nos.	Lot. Nos.	Concentrations used
Key antibodies				
Ant-growth-associated protein 43 (GAP43)	Santa Cruz Biotechnology	sc-17790	J0920	Immunoblotting (IB), 1:5000
Anti-b3 tubulin	Santa Cruz Biotechnology	sc-51670	H2721	IB, 1:500
Anti-Arf6	Santa Cruz Biotechnology	sc-7971	E0919	IB, 1:50
Anti-FE65	Santa Cruz Biotechnology	sc-398389	H2117	IB, 1:50
Anti-green fluorescent protein (GFP)	MBL	598	005	Immunofluorescence (IF), 1:500; IB, 1/500
Anti-Tau	Santa Cruz Biotechnology	sc-121796	J2524	IF, 1:200; IB, 1/500
Anti-actin (also called pan-β type actin)	MBL	M177-3	007	IB, 1:5000
Anti-IgG (H+L chain) (Rabbit) pAb-HRP	MBL	458	353	IB, 1:5000
Anti-IgG (H+L chain) (Mouse) pAb-HRP	MBL	330	365	IB, 1:5000
Alexa Fluor TM 488 goat anti-mouse IgG (H+L)	Thermo Fisher Scientific	A11001	774-9040	IF, 1:500
Alexa Fluor TM 594 goat anti-mouse IgG (H+L)	Thermo Fisher Scientific	A11005	226-8383	IF, 1:500
Alexa Fluor TM 488 goat anti-rabbit IgG (H+L)	Thermo Fisher Scientific	A11008	075-1094	IF, 1:500
Alexa Fluor TM 594 goat anti-rabbit IgG (H+L)	Thermo Fisher Scientific	A11012	201-8240	IF, 1:500
Recombinant DNAs				
pCMV-SV40ori	A control construct was generated using Cat. No. 72035 (Addgene) as a template	n.d.	N/A	1.25 mg of DNA per 6 cm dish
pCMV-SV40ori-mouse Sema5A-His	Addgene	72035	N/A	1.25 mg of DNA per 6 cm dish
pCMV-SV40ori-mouse Sema5A (R676C) -His	Mutation was performed using Cat. No. 72035 (Addgene) as a template	N/A	N/A	1.25 mg of DNA per 6 cm dish
pcDNA3.1-mKate (also known as RFP)-human ELMO2	generated in this study	N/A	N/A	1.25 mg of DNA per 6 cm dish
NLS-RfxCas13d-NLS (mamalian cell expression plasmid for Cas13)	Addgene	109049	N/A	1.25 mg of DNA per 6 cm dish
pSIN-mU6	Takara Bio (discontinued product)	N/A	N/A	1.25 mg of DNA per 6 cm dish
pSIN-mU6-gRNA for Luciferase (control gRNA, 105), which contains complementary 22 bases from base 105 of the firefly luciferase sequence (5'-GCACCCGTGCAAAAATGCAGGGGTCTAAAACATCCTCTAGAGGATAGAATGGCTTTTTT-3' is inserted into BamHI and ClaI multiple cloning sites)	generated in this study	N/A	N/A	1.25 mg of DNA per 6 cm dish
pSIN-mU6-gRNA for Arf6 (169), which contains complementary 22 bases from base 169 of the mouse Arf6 sequence (5'-GCACCCGTGCAAAAATGCAGGGGTCTAAAACCATCCCACACGTTGAACTTGACTTTTTT-3' is inserted into BamHI and ClaI multiple cloning sites)	generated in this study	N/A	N/A	1.25 mg of DNA per 6 cm dish
pSIN-mU6-gRNA for Arf6 (345), which contains complementary 22 bases from base 345 of the mouse Arf6 sequence (5'-GCACCCGTGCAAAAATGCAGGGGTCTAAAACGTTGGCGAAGATGAGGATGATGTTTTTT-3' is inserted into BamHI and ClaI multiple cloning sites)	generated in this study	N/A	N/A	1.25 mg of DNA per 6 cm dish
pSIN-mU6-gRNA for FE65 (1011), which contains complementary 22 bases from base 1011 of the mouse FE65 sequence (5'-GCACCCGTGCAAAAATGCAGGGGTCTAAAACCTGAGCTGGGAAGGACAATGTCTTTTTT-3' is inserted into BamHI and ClaI multiple cloning sites)	generated in this study	N/A	N/A	1.25 mg of DNA per 6 cm dish
pSIN-mU6-gRNA for FE65 (1182), which contains complementary 22 bases from base 1182 of the mouse FE65 sequence (5'-GCACCCGTGCAAAAATGCAGGGGTCTAAAACGAGCTGGCGGATACAATTGTTGTTTTTT-3' is inserted into BamHI and ClaI multiple cloning sites)	generated in this study	N/A	N/A	1.25 mg of DNA per 6 cm dish
pcDNA3.1(+)-eGFP-human FE65 (1-150 amino acids), which specifically interacts with ELMO2	GenScript	J196YHL120-4	TJ846140	1.25 mg of DNA per 6 cm dish
pEGFP-C1 (mamalian cell GFP expresssion plasmid)	Takara Bio (discontinued product)	N/A	N/A	1.25 mg of DNA per 6 cm dish